these materials. Some of the effects may be indicative of the solvent-casting procedures used in preparing the blends and may be related to the fact that the measurements were taken below the glass temperature of the polystyrene blocks. Nevertheless, these results illustrate the sensitivity of energy transfer to the phase behavior of these systems.
(25) A forerunner of the two-state energy-transfer model first described in ref 2 is the two-state excimer fluorescence model by Gelles and Frank (Gelles, R.; Frank, C. W. *Macromolecules* **1982**, *15*, 1486).
(26) In the particular case of Figure 5b, it is relatively easy to estimate a value of the y intercept with small error. (It was taken to be 0.475.) However, readers who may be doing similar studies are warned against trying to reduce the error by obtaining I_A/I_D at high block copolymer concentrations, resulting in data very close to the y intercept in a plot of I_A/I_D vs $1/W$. At high block copolymer concentrations, radiative energy transfer, not to mention a change in gross microphase-separated structure, may invalidate the approach defined and used in this study. Care was used in the present study to employ concentrations low enough to minimize such effects but high enough to allow a reasonable estimate of the y intercept in Figure 5b.
(27) For the IS10/11 systems studied here, f_A/f_D was taken to be 0.11_4 as in ref 2. Φ_A/Φ_D (actually not true quantum yields as the left-hand side of eq 4 is a ratio of intensities rather than quantum yields) was determined in ref 2 to be 3.95 in a cyclohexane/heptane solution; in the absence of accessible fluorescence data below the cmc in a blend of IS10/11 in 9000 MW PI, it was assumed that 3.95 was a reasonable estimate for Φ_A/Φ_D in the blend.
(28) Major, M. D. Ph.D. Thesis, Northwestern University, 1989.
(29) Turro, N. J. *Modern Molecular Photochemistry*; Benjamin/Cummings Publishing Co. Inc.: Reading, MA, 1978.
(30) Lakowicz, J. R. *Principles of Fluorescence Spectroscopy*; Plenum Press: New York, 1983.
(31) Cheikh Larbi, F. B.; Malone, M. F.; Winter, H. H.; Halary, J. L.; Leviet, M. H.; Monnerie, L. *Macromolecules* **1988**, *21*, 3534.
(32) Fayt, R.; Jerome, R.; Teyssie, P. *J. Polym. Sci., Polym. Phys. Ed.* **1981**, *19*, 1269; **1982**, *20*, 2209.
(33) Jerome, R.; Teyssie, P. *J. Polym. Sci., Polym. Phys. Ed.* **1986**, *24*, 25.
(34) Poddubnyi, I. Ya.; Ehrenberg, E. G. *J. Polym. Sci.* **1962**, *57*, 545.

Registry No. PI, 9003-31-0; (isoprene)(styrene) (block copolymer), 105729-79-1.

Flow and Diffusion through Random Suspensions of Aggregated Rods: Application to Proteoglycan Solutions

Christopher G. Phillips

Physiological Flow Studies Unit and Department of Mathematics, Imperial College, Prince Consort Road, London SW7 2AZ, England

Kalvis M. Jansons*

Department of Mathematics, University College London, Gower Street, London WC1E 6BT, England. *Received June 12, 1989*

ABSTRACT: Flow and point-solute diffusion through random distributions of rods and model rod assemblages with small volume fraction is considered. The effect of steric interactions on the rod orientation distribution in the assemblages is calculated. The method of averaged equations is used to calculate the effective diffusion coefficient and the flow permeability in both distributions of rods and rod assemblages. We discuss the application to biopolymer aggregates, particularly proteoglycans, and consider dependence on polymer concentration and the effect of aggregation.

1. Introduction

As a model for transport in biopolymer solutions, we consider flow and diffusion in random distributions of rods and rod assemblages with small volume fraction.

Long-chain, highly charged polyions have an important effect on the physicochemical properties of connective tissue, which are reviewed by Grodzinsky.[1] The polyions influence the diffusion of both small ions and larger solutes and resist the flow of water, enhancing the tissue's ability to withstand rapid deformation. The fixed charges on the polymers produce a large swelling pressure, giving tissues such as cartilage a load-bearing ability, and cause electrokinetic phenomena such as electroosmosis and streaming potentials, in which electric fields and ion fluxes are coupled to pressure gradients and solvent flow.

* Author to whom correspondence should be addressed.

The glycosaminoglycans (GAGs) are an important component of connective tissue, often occurring in aggregates known as proteoglycans (PGs). There are two stages of aggregation: first, GAG side chains (chondroitin sulfate and keratan sulfate) are attached to a core protein to form a "PG monomer", and second, PG monomers are bound to a hyaluronate molecule to form a PG aggregate. The PG aggregate has a complicated branched structure (see Figure 1) and can contain up to 40 000 GAG side chains. Although the function of PGs is not well understood, the resulting inhomogeneity in the GAG concentration has a potentially large effect on the properties of the tissue. For example, the large variation of the viscosity of PG solutions with the proportion of monomers aggregated has been measured experimentally.[2]

In this study the GAG side chains are idealized as cylinders. Several workers have used the ad hoc rod-in-cell model to investigate flow[3,4] and point-solute diffusion[5]

0024-9297/90/2223-1717$02.50/0

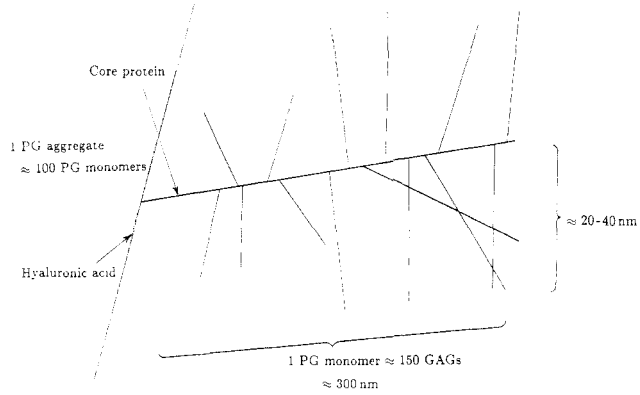

Figure 1. Schematic diagram of proteoglycan structure.

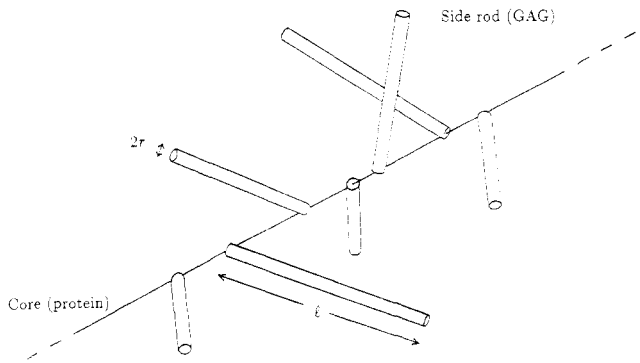

Figure 2. Model of a rod assemblage.

in random distributions of circular cylinders. Averaged transport properties in random distributions of obstacles can be obtained rigorously by the method of averaged equations, reviewed by Hinch.[6] This has been applied to flow[7] and diffusion[8] in distributions of aligned or isotropically oriented cylinders with small volume fraction and to small-ion diffusion parallel to aligned cylinders.[9] The nonlinear interaction between flow and diffusion has also been considered;[10] as discussed in section 5, this interaction is negligible in typical biopolymer solutions.

Here, we use averaged equations to calculate flow and diffusion in random distributions of uncharged cylinders with small volume fraction. The effect of aggregation is investigated by comparison with a random distribution of simple assemblages of cylinders. We describe these as assemblages rather than aggregates because the results are applied to both levels of aggregation in a PG solution, with the assemblages representing either PG monomers or PG aggregates. The model assemblage is shown in Figure 2. The side rods, cylinders of length l, are attached by one end to the core, represented by a straight line, with attachment points randomly distributed with uniform number density n. We consider cylinders with arbitrary convex cross section, restricting attention to circular cylinders in sections 3 and 4. For noncircular cylinders whose cross section has perimeter s, we define an equivalent radius $r = s/2\pi$. In section 2 we calculate the leading-order effect on the side-rod orientation distribution due to steric interactions between side rods. In section 3 we determine the effective diffusivity of a point solute in a random distribution of cylinders and in a random distribution of assemblages with small volume fractions. The flow resistance in a random distribution of fixed cylinders and a random distribution of fixed assemblages is calculated in section 4. The results show the effect of aggregation on the diffusion of small ions and larger solutes and on flow resistance. The application to PG solutions is discussed in section 5.

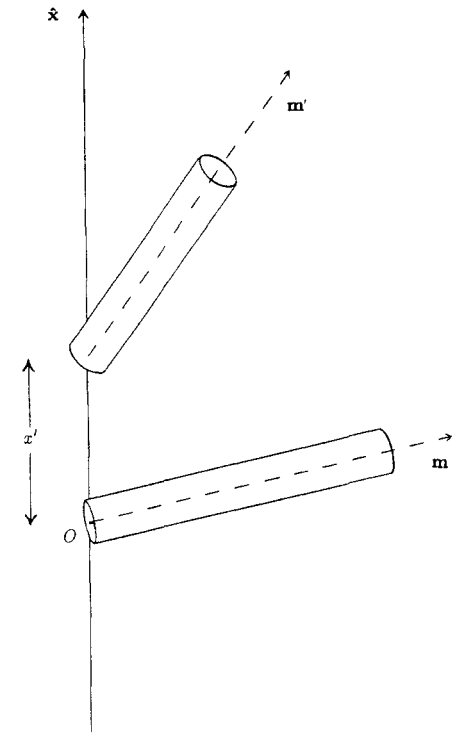

Figure 3. Defining diagram for side-rod calculation.

2. Cylinder Orientation Distribution

In this section, we calculate the leading-order correction to the cylinder orientation distribution due to steric interactions between cylinders, i.e. due to the constraint that cylinders do not intersect, when the cylinders have arbitrary convex cross section. Consider an ensemble of realizations of the assemblage with the cylinders distributed independently, with a uniform number density of attachments and isotropic orientation distribution, and remove all realizations in which cylinders intersect. We seek the orientation distribution in the remaining realizations. Note that in this section we do not assume that the cylinders are circular, only that they have convex cross section.

Denoting the direction of a cylinder axis by the unit vector $\mathbf{m}$, the orientation probability density function $q_0(\mathbf{m})$ in the absence of interactions is

$$q_0(\mathbf{m}) = 1 \tag{1}$$

where orientation space has total measure unity. We calculate the leading-order correction to (1) due to pair interactions between cylinders assuming the effect of steric interactions is small. (This is so provided the parameter δ defined by (7) below is small.) Define the probability density function $q(\mathbf{m}|x',\mathbf{m}')$ for the orientation $\mathbf{m}$ of a cylinder, given that there is another cylinder whose attachment point has displacement x' and whose axis is parallel to $\mathbf{m}'$ (see Figure 3). Then the leading-order correction to q_0 is

$$q_1(\mathbf{m}) = n \int \int \{q(\mathbf{m}|x',\mathbf{m}') - 1\}\, dx'\, d\mathbf{m}' \tag{2}$$

Since there is no steric interaction between cylinders with attachment points more than $2l$ apart, the integrand is zero for $|x'| > 2l$.

Define $\chi(\mathbf{m}|x',\mathbf{m}')$ to be 1 when the cylinders intersect and 0 otherwise. For convex bodies χ is the Euler characteristic of the intersection. The probability $f(x',\mathbf{m}')$ that

a cylinder with isotropic orientation distribution intersects a second cylinder with position and orientation $(x',\mathbf{m}')$ is

$$f(x',\mathbf{m}') = \int \chi(\mathbf{m}|x',\mathbf{m}')\, d\mathbf{m} \tag{3}$$

Since the integral of $q(\mathbf{m}|x',\mathbf{m}')$ with respect to $\mathbf{m}$ is unity

$$q(\mathbf{m}|x',\mathbf{m}') = \frac{1-\chi(\mathbf{m}|x',\mathbf{m}')}{1-f(x',\mathbf{m}')} \tag{4}$$

Consider cylinders of length l and convex cross section with perimeter $s \ll l$. To leading order, intersecting configurations of cylinders where the angle between the axes is of order sl^{-1} can be ignored. The measure of the remaining intersecting configurations is proportional to the width of the cross section averaged over orientations of the cross section. Since the cross section is convex the mean width is[11] s/π. Provided $s(x'|\hat{\mathbf{x}} \times \mathbf{m}'|)^{-1}$ is small, the probability of intersection, f, is also small. Substituting (4) into (2) and using the fact that f is small over most of the range of integration and the relationship $\chi(\mathbf{m}|x',\mathbf{m}') = \chi(-\mathbf{m}'|x',-\mathbf{m})$ give

$$q_1(\mathbf{m}) = Q - n\int f(x',-\mathbf{m})\, dx' + O(ns|\hat{\mathbf{x}} \times \mathbf{m}|^{-1}) \tag{5}$$

as $ns|\hat{\mathbf{x}} \times \mathbf{m}|^{-1} \to 0$, where Q is to be chosen so that q_1 integrates to zero. A leading-order calculation for f gives

$$n\int f(x',-\mathbf{m})\, dx' = \frac{ns \ln (ls^{-1})}{\pi^2|\hat{\mathbf{x}} \times \mathbf{m}|} + O\left(\frac{ns}{|\hat{\mathbf{x}} \times \mathbf{m}|}\right) \tag{6}$$

as $ns|\hat{\mathbf{x}} \times \mathbf{m}|^{-1}, sl^{-1} \to 0$. Define the dimensionless parameter

$$\delta = ns \ln (ls^{-1}) \tag{7}$$

From (5) and (6) the perturbed cylinder orientation distribution is

$$q(\mathbf{m}) = 1 + \frac{\delta}{2\pi}\left(1 - \frac{2}{\pi|\hat{\mathbf{x}} \times \mathbf{m}|}\right) + O\left(\delta^2, \frac{ns}{|\hat{\mathbf{x}} \times \mathbf{m}|}\right) \tag{8}$$

as δ, $ns|\hat{\mathbf{x}} \times \mathbf{m}|^{-1}$, $sl^{-1} \to 0$. The correction term in (8) becomes large when $\mathbf{m}$ is nearly parallel to the core, i.e. when $|\hat{\mathbf{x}} \times \mathbf{m}|$ is small, but the singularity is integrable. The parameter δ expresses the strength of steric interactions: the orientation distribution is nearly isotropic if $\delta \ll 1$ but favors orientations perpendicular to the core for larger δ.

3. Diffusion

3.1. Distributions of Permeable Cylinders. In this subsection the diffusion of a point solute in a random distribution of obstacles with small volume fraction c is considered. When the obstacles are infinite circular cylinders, the leading-order contribution to the effective diffusion coefficient is calculated.

We consider a homogeneous distribution of well-separated obstacles with an arbitrary orientation distribution. The diffusivity within the obstacles is allowed to be anisotropic and to vary with position. Denote the tensor diffusion coefficient by $\mathbf{D}$, so that the solute flux density $\mathbf{J}$ is

$$\mathbf{J} = -\mathbf{D}\cdot\nabla F \tag{9}$$

where F is the solute number density. The continuity equation is

$$\nabla\cdot(\mathbf{D}\cdot\nabla F) = 0 \tag{10}$$

Assume the diffusivity outside the obstacles to be isotropic, so without loss of generality $\mathbf{D} = 1$, where 1 is the identity tensor.

Denote by $\langle\cdot\rangle$ the ensemble average over realizations of the obstacle distribution. Define the effective diffusivity tensor $\mathbf{D}_e$ for a uniform averaged concentration gradient $\langle\nabla F\rangle$ so that

$$\langle\mathbf{J}\rangle = -\mathbf{D}_e\cdot\langle\nabla F\rangle \tag{11}$$

Define I to be 1 within an obstacle and 0 otherwise. Then at position $\mathbf{r}$

$$\begin{aligned}\mathbf{D}_e\cdot\langle\nabla F\rangle &= \langle\mathbf{D}\cdot\nabla F\rangle \\ &= \langle\nabla F + I(\mathbf{D}-1)\cdot\nabla F\rangle \\ &= \langle\nabla F\rangle + c\langle(\mathbf{D}-1)\cdot\nabla F\rangle_I\end{aligned} \tag{12}$$

where $\langle\cdot\rangle_I$ is an average over realizations for which $\mathbf{r}$ lies inside an obstacle. If the internal diffusivity is uniform and isotropic, i.e. $\mathbf{D} = d\mathbf{1}$ within the obstacles for some positive d, then

$$\mathbf{D}_e\cdot\langle\nabla F\rangle = \langle\nabla F\rangle + c(d-1)\langle\nabla F\rangle_I \tag{13}$$

Now restrict attention to circular cylinders. The leading-order contribution to $\mathbf{D}_e$ is obtained from the solution F_0 for diffusion past an isolated cylinder where ∇F_0 tends to a uniform value $\mathbf{G}_0$ far from the cylinder. This gives

$$\nabla F_0 = \begin{cases}\left[\mathbf{mm} + \frac{2}{1+d}(1-\mathbf{mm})\right]\cdot\mathbf{G}_0 & (\rho < \rho_0) \\ \left[1 + \frac{1-d}{1+d}\left(\frac{\rho_0}{\rho}\right)^2(1-\mathbf{mm})\right]\cdot\mathbf{G}_0 & (\rho > \rho_0)\end{cases} \tag{14}$$

where $\mathbf{m}$ is a unit vector parallel to the cylinder axis, ρ is the distance from the axis, and ρ_0 is the radius of the cylinder. Setting $\mathbf{G}_0$ equal to $\langle\nabla F\rangle$ and ρ_0 equal to r and substituting into (13) gives

$$\mathbf{D}_e = 1 + c(d-1)(d+1)^{-1}((\mathbf{d}\text{-}1)\langle\mathbf{mm}\rangle + 21) + O(c^2) \tag{15}$$

as $c \to 0$, where the average $\langle\mathbf{mm}\rangle$ is over cylinder orientations. If, instead of the system being homogeneous, $\langle\nabla F\rangle$ and c vary on a length scale L much larger than the radius of the cylinders

$$\langle\mathbf{J}\rangle = -\mathbf{D}_e\cdot\langle\nabla F\rangle(1 + O(crL^{-1})) \tag{16}$$

as $c, rL^{-1} \to 0$. If the system is homogeneous, but the cylinders have finite length l much larger than their radius, eq 16 applies with $L = l$.

In section 3.2 we consider assemblages with impermeable side rods, so that $d = 0$ and

$$\mathbf{D}_e = \mathbf{1} - c(21 - \langle\mathbf{mm}\rangle) + O(c^2) \tag{17}$$

as $c \to 0$. In an isotropic distribution of impermeable cylinders, $\langle\mathbf{mm}\rangle$ is isotropic with a trace of 1, so $\langle\mathbf{mm}\rangle = (1/3)\mathbf{1}$. Thus

$$\mathbf{D}_e = (1 - (5/3)c + O(c^2))\mathbf{1} \tag{18}$$

as $c \to 0$. In the Appendix we give other special cases of (15) together with the c^2 term when the cylinders are aligned.[8]

3.2. Distributions of Assemblages. The effective diffusion coefficient for a point solute in a homogeneous, isotropic distribution of assemblages with small volume fraction is calculated. The volume fraction within the assemblages occupied by side rods is also assumed to be small. The ensemble average over realizations of the distribution is performed in two stages: first, for each realization of the cores of the assemblages, we average over all positions and orientations of side rods, and sec-

ond, we average over realizations of the cores. The effective diffusivity is derived from an equation of the form of (12), with c replaced by the volume fraction ϕ of assemblages and with $\langle\cdot\rangle_I$ replaced by an average over realizations in which the position $\mathbf{r}$ lies inside an assemblage, i.e. within a distance l of its core.

For a quantity $a(\rho)$ varying with the distance ρ from the core of an assemblage, denote the spatial average over the interior by

$$\bar{a} = 2l^{-2}\int_0^l a(\rho)\rho\, d\rho \tag{19}$$

Then the volume fraction of an assemblage occupied by side rods is $\bar{c} = nr^2 l^{-1}$. From (17), the first stage of averaging gives an effective diffusion coefficient

$$\mathbf{D}(\rho) = \mathbf{1} + \bar{c}\mathbf{E}(\rho) + O(c^2) \tag{20}$$

as $c \to 0$, where

$$\mathbf{E}(\rho) = -\frac{c}{\bar{c}}[2\mathbf{1} - \langle \mathbf{mm}\rangle_S] \tag{21}$$

in which $\langle\cdot\rangle_S$ is an average over realizations of the side rods for a fixed position and orientation of the core. Note that c is not small in a region near the core where ρ is of order nr^2. Within the assemblage, $\langle\nabla F\rangle_S$, c, and $\langle \mathbf{mm}\rangle_S$ vary on the length scale ρ. The resulting small corrections are estimated in (23) below.

Since $\bar{c}$ is small, $\langle F\rangle_S$ is only slightly perturbed by the assemblage, that is

$$\langle\nabla F\rangle_S = \langle\nabla F\rangle + O(\bar{c},\bar{c}^2 l^2\rho^{-2}) \tag{22}$$

as $\bar{c},\bar{c}l\rho^{-1} \to 0$. The average replacing $\langle\cdot\rangle_I$ in (12) is

$$\langle(\mathbf{D} - \mathbf{1})\cdot\nabla F\rangle_I = \bar{c}\langle\mathbf{E}\rangle_I\cdot\langle\nabla F\rangle(1 + O(\bar{c},\phi,rl^{-1})) \tag{23}$$

as $\bar{c},\phi,rl^{-1} \to 0$. The first two error terms come from the $O(\bar{c})$ error in (22) and from interactions between different assemblages. The other error term is obtained by putting $L = \rho$ in (16) to allow for the inhomogeneity of the assemblages on the length scale ρ. The relative error due to the core region is $O(\bar{c}^2)$.

The average $\langle\mathbf{E}\rangle_I$ is evaluated as follows. Since the distribution of assemblages is homogeneous, the average $\langle\cdot\rangle_I$ is equivalent to an average over orientations of the core for fixed ρ, followed by the spatial average defined by (19). Since the orientation distribution of the core is isotropic, the first average replaces $\langle \mathbf{mm}\rangle_S$ in (21) by $(1/3)\mathbf{1}$. The spatial average gives

$$\langle\mathbf{E}\rangle_I = -(5/3)\mathbf{1} \tag{24}$$

Note that $\langle\mathbf{E}\rangle_I$ does not depend on the form of the spatial variation of c and $\langle \mathbf{mm}\rangle_S$. From (12) and (23), the effective diffusion coefficient for the distribution of assemblages is

$$\mathbf{D}_e = (1 - (5/3)\phi\bar{c} + \phi\bar{c}O(\phi,\bar{c},rl^{-1}))\mathbf{1} \tag{25}$$

as $\phi,\bar{c},rl^{-1} \to 0$. Comparing with (18), since $\phi\bar{c}$ is the total volume fraction of side rods in the distribution, to first order in $\phi\bar{c}$ the effective diffusivity is the same as if the side rods were homogeneously and isotropically distributed.

3.3. Spherical Solute of Nonzero Radius. The effective diffusion coefficient (18), for a point solute in a random isotropic distribution of impermeable cylinders with small volume fraction, can also be applied to the diffusion of a spherical solute of nonzero radius in both distributions of cylinders and assemblages.

Consider a spherical solute of radius $\mathcal{R}$ in a distribution of cylinders of length l and radius r with volume fraction c. Under the following conditions, the leading-order effect on the diffusivity is the same as for a point solute in a distribution of cylinders of length l and radius $\mathcal{R}$ with volume fraction $c' = \mathcal{R}^2 r^{-2} c$. The conditions are that $r \ll \mathcal{R}$, so that hydrodynamic effects are negligible and that $\mathcal{R} \ll l$, so that the length of the cylinders is still much greater than their radius. From (18) we find

$$\mathbf{D}_e = (1 - (5/3)c' + c'O(c',\mathcal{R}l^{-1},r\mathcal{R}^{-1}))\mathbf{1} \tag{26}$$

as $c',\mathcal{R}l^{-1},r\mathcal{R}^{-1} \to 0$. The empirical theory of Ogston et al.[12] for the diffusion of a ball in a random distribution of cylinders gives, in our notation, $\mathbf{D}_e = \exp\{-c'^{1/2}\}\mathbf{1}$. This does not agree with (26) when c' is small; further, it should be noted that the theory does not have the correct asymptotic behavior in any limit.

Similarly, under the following conditions, the leading-order effect on the diffusion coefficient of a spherical solute of radius $\mathcal{R}$ in a distribution of assemblages with volume fraction ϕ is the same as for a point solute in a distribution of impermeable cylinders of radius l with volume fraction ϕ. The conditions are that $\mathcal{R} \ll l$, so that the solute is much smaller than the assemblage radius and that $\mathcal{R} \gg (l/n)^{1/2}$; i.e., the solute radius is much larger than the typical spacing of side-rod ends, so that the solute cannot penetrate the assemblage. Then

$$\mathbf{D}_e = (1 - (5/3)\phi + \phi O(\phi, l\mathcal{R}^{-1},\mathcal{R}(l/n)^{1/2}))\mathbf{1} \tag{27}$$

as $\phi,l\mathcal{R}^{-1},\mathcal{R}(l/n)^{1/2} \to 0$.

Substituting $c' = \mathcal{R}^2 r^{-2}\phi\bar{c}$ in (26) gives the effective diffusivity in a homogeneous, isotropic distribution of side rods with volume fraction $\phi\bar{c}$. The conditions required for (26) and (27) are that

$$(l/n)^{1/2} \ll \mathcal{R} \ll \min((l/n\phi)^{1/2}, l) \tag{28}$$

The decrease in diffusivity in (26) is much larger than in (27), so the diffusivity of a solute whose radius satisfies (28) is larger in the distribution of assemblages than in the distribution of side rods with the same overall volume fraction.

4. Flow Permeability

4.1. Impermeable Fixed Cylinders. We calculate the averaged flow permeability of a random distribution of fixed, impermeable circular cylinders with small volume fraction and arbitrary orientation distribution. Both infinite and finite cylinders are considered.

To average the governing equation for flow, it is convenient to extend the definitions of the fluid velocity $\mathbf{u}$ and pressure p to cover all space (though we do not attach any physical significance to $\mathbf{u}$ and p within the cylinders). For any realization of the cylinder distribution, define $\mathbf{u}(\mathbf{r}) = 0$ and $p(\mathbf{r}) = \langle p(\mathbf{r})\rangle_0$ within the cylinders, where $\langle\cdot\rangle_0$ is the ensemble average over realizations in which $\mathbf{r}$ is not inside a cylinder. To cancel the resulting singular parts of $\nabla^2\mathbf{u}$ and ∇p, we also introduce a force density, $\mathbf{f}$ (a generalized function), singular at the cylinder surfaces and zero elsewhere. Then for any realization

$$0 = -\nabla p + \mu\nabla^2\mathbf{u} + (I\nabla\langle p\rangle + \mathbf{f}) \tag{29}$$

where $I = 1$ within a cylinder and 0 otherwise. Since within a cylinder $\nabla p = \nabla\langle p\rangle_0 = \nabla\langle p\rangle$, the terms containing p cancel there, as required.

Consider a spatially homogeneous system, where $\langle\mathbf{u}\rangle$ and $\nabla\langle p\rangle$ are uniform. In the ensemble average of (29),

$\nabla^2\langle\mathbf{u}\rangle = 0$ and, since the average of I is c, $\langle I\nabla\langle p\rangle\rangle = c\nabla\langle p\rangle$. As (29) is linear, $\langle\mathbf{f}\rangle$ depends linearly on $\langle\mathbf{u}\rangle$, so we can define the resistance tensor $\mathbf{K}$ so that

$$\langle\mathbf{f}\rangle = (1-c)\nabla\langle p\rangle = -\mathbf{K}\cdot\langle\mathbf{u}\rangle \tag{30}$$

When the cylinder orientation distribution is isotropic, $\mathbf{K} = \alpha_0\mathbf{1}$, where α_0^{-1} is the flow permeability or Darcy constant.

Define the subset S of realizations that include a test cylinder with some specified position and orientation, and denote the ensemble average over S by $\langle\cdot\rangle_S$. The averaged force density $\langle\mathbf{f}\rangle$ is obtained by calculating the averaged force per unit length exerted by the test cylinder. The singular force at the surface of the cylinder cancels the singular parts of $\nabla\langle p\rangle_S$ and $\nabla^2\langle\mathbf{u}\rangle_S$. However, for $\mathbf{r}$ on the surface of the cylinder, the singular parts of $\nabla\langle p\rangle_S$ at $\mathbf{r}$ and $-\mathbf{r}$ cancel. Therefore the contribution from the discontinuity of $\nabla\langle p\rangle_S$ at the surface integrates to zero, and we need consider only the velocity gradients at the surface. The ensemble average over S of (29) is

$$0 = -\nabla\langle p\rangle_S + \mu\nabla^2\langle\mathbf{u}\rangle_S + (\langle I\rangle_S\nabla\langle p\rangle + \langle\mathbf{f}\rangle_S) \tag{31}$$

where far from the test cylinder $\langle\mathbf{f}\rangle_S \to -\mathbf{K}\cdot\langle\mathbf{u}\rangle$ and $\langle I\rangle_S \to c$.

Let α be the size of a typical element of $\mathbf{K}$. Below we solve (31) at leading order for $\alpha r^2\mu^{-1} \ll 1$ and derive an implicit equation for α from (30). The value thus determined does satisfy $\alpha r^2\mu^{-1} \ll 1$, so the solution is self-consistent. The condition $\alpha r^2\mu^{-1} \ll 1$ means that the length scale on which the resistance term in (31) is important is much larger than the cylinder radius r. Thus the problem can be solved by using matched asymptotic expansions with an outer region with the resistance length scale $(\mu/\alpha)^{1/2}$ and an inner region with length scale r. In the inner region the terms in parentheses in (31) are small and do not affect the leading-order solution. Matching to the outer region using an intermediate variable shows that to obtain the leading-order velocity gradients at the surface of the test cylinder we can replace the bracketed terms by $-\alpha\langle\mathbf{u}\rangle_S$. Therefore consider

$$0 = -\nabla\langle p\rangle_S + \mu\nabla^2\langle\mathbf{u}\rangle_S - \alpha\langle\mathbf{u}\rangle_S \tag{32}$$

with $\langle\mathbf{u}\rangle_S = 0$ at the test cylinder surface and $\langle\mathbf{u}\rangle_S \to \mathbf{u}_\infty$ far away, for some uniform $\mathbf{u}_\infty$. This is the Debye–Brinkman equation, which has been applied[13] to the flow permeability of isotropic distributions of cylinders.

Since (32) is linear, its solution can be decomposed into two parts: (i) for parallel flow with $\mathbf{u} \to \mathbf{u}_\parallel$ far from the cylinder and (ii) for perpendicular flow with $\mathbf{u} \to \mathbf{u}_\perp$. For parallel flow, to leading order the force exerted by the test cylinder per unit length is

$$\mathbf{F}_\parallel \sim -\frac{4\pi\mu\mathbf{u}_\parallel}{\ln(\alpha r^2\mu^{-1})} \tag{33}$$

as $\alpha r^2\mu^{-1} \to 0$. For perpendicular flow it is

$$\mathbf{F}_\perp \sim -\frac{8\pi\mu\mathbf{u}_\perp}{\ln(\alpha r^2\mu^{-1})} \tag{34}$$

as $\alpha r^2\mu^{-1} \to 0$. Averaging over orientations of the test cylinder

$$\mathbf{K}\cdot\langle\mathbf{u}\rangle = -\langle\mathbf{f}\rangle \sim \frac{c}{\pi r^2}\beta(2\mathbf{1} - \langle\mathbf{mm}\rangle)\cdot\langle\mathbf{u}\rangle \tag{35}$$

as $\alpha r^2\mu^{-1} \to 0$, where

$$\beta = \frac{4\pi\mu}{\ln(\alpha r^2\mu^{-1})} \tag{36}$$

and $\langle\mathbf{mm}\rangle$ is an average over cylinder orientations. From (35), since α is the size of a typical element of $\mathbf{K}$, we can choose $\alpha = c\beta r^{-2}$. Then (36) is an implicit equation for β, whose solution gives

$$\mathbf{K} = \frac{4\mu c}{r^2\ln c^{-1}}(2\mathbf{1} - \langle\mathbf{mm}\rangle)\left[1 + O\left(\frac{\ln\ln c^{-1}}{\ln c^{-1}}\right)\right] \tag{37}$$

as $c \to 0$. This is consistent with the condition that $\alpha r^2\mu^{-1} \ll 1$, used above.

For an isotropic distribution of cylinders, $\mathbf{K} = \alpha_0\mathbf{1}$, where

$$\alpha_0 = \frac{20\mu c}{3r^2\ln c^{-1}}\left[1 + O\left(\frac{\ln\ln c^{-1}}{\ln c^{-1}}\right)\right] \tag{38}$$

as $c \to 0$. This agrees at leading order with earlier derivations using rod-in-cell models,[3,4] the Debye–Brinkman equation[13] and averaged equations.[10] When the cylinders are parallel, (37) agrees with earlier results.[7,10,13]

As in section 3.1, the assumption of homogeneity can be relaxed. The length scale on which resistance becomes important is $r(c^{-1}\ln c^{-1})^{1/2}$, which is much larger than the radius of the cylinders. The effective resistance coefficient (37) applies, with the same relative error, provided c, $\langle\mathbf{mm}\rangle$, $\langle\mathbf{u}\rangle$, and $\langle\nabla p\rangle$ do not vary on a scale much smaller than the resistance length scale. Equation 37 also applies for cylinders of finite length l unless $l \ll r(c^{-1}\ln c^{-1})^{1/2}$. Apart from a logarithmic factor, this condition means l is much smaller than the typical spacing of cylinders, and the cylinders behave as isolated obstacles. Using the drag on a finite slender cylinder at zero Reynolds number,[14] a calculation similar to that of Howells[7] shows that the flow resistance for $l \ll r(c^{-1}\ln c^{-1})^{1/2}$ is

$$\mathbf{K} = \frac{2\mu c}{r^2\ln(lr^{-1})}(2\mathbf{1} - \langle\mathbf{mm}\rangle)[1 + O(\ln(lr^{-1}))^{-1}] \tag{39}$$

as $c, rl^{-1} \to 0$. When c is comparable with $r^2l^{-2}\ln c^{-1}$, this agrees with (37) at leading order. In this case the resistance length scale is $r(c^{-1}\ln(lr^{-1}))^{1/2}$. Equation 39 applies when averaged quantities vary with position provided the length scale of the variation is not much smaller than the resistance length scale.

4.2. Fixed Assemblages. In this subsection we calculate the averaged flow permeability of a homogeneous, isotropic distribution of fixed assemblages with small volume fraction ϕ. The side rods are assumed to be fixed and to occupy a small volume fraction within the assemblages. As in section 3.2, we average over realizations of the side rods and then over realizations of the cores. Denote by S the set of realizations that include a test assemblage whose core has a specified position and orientation. The averaged flow within the test assemblage is governed by

$$0 = -\nabla\langle p\rangle_S + \mu\nabla^2\langle\mathbf{u}\rangle_S - \mathbf{K}\cdot\langle\mathbf{u}\rangle_S \tag{40}$$

where $\mathbf{K}$ is given by (37) or (39) as appropriate. Note that the $\langle I\rangle_S\nabla\langle p\rangle$ term in (31) is of higher order than the error term in (37) for small $\bar{c}$.

As in section 4.1, we calculate the averaged force exerted by the test assemblage. Now, however, there is a finite resistance within the assemblage, and the average of $-\mathbf{K}\cdot\langle\mathbf{u}\rangle$ within the assemblage replaces the singular force at the surface of the impermeable test cylinder. (Note that the result for the impermeable cylinders could alter-

natively be obtained from the limit in which uniform internal resistance tends to infinity, though the direct approach of section 4.1 is more straightforward.)

Define the parameter R by nondimensionalizing a typical value of the resistance within an assemblage with respect to the assemblage radius l. Thus

$$R = \begin{cases} \dfrac{l^2\bar{c}}{2r^2 \ln (lr^{-1})} = \dfrac{nl}{2 \ln (lr^{-1})} & \text{for } nl \ll \ln \bar{c}^{-1} \\ \dfrac{l^2\bar{c}}{r^2 \ln \bar{c}^{-1}} = \dfrac{nl}{\ln \bar{c}^{-1}} & \text{for } nl \gg \ln \bar{c}^{-1} \end{cases} \quad (41)$$

The latter case is appropriate when the length of the cylinder is much greater than the resistance length scale, and the former case when it is much smaller, so that the cylinders appear as isolated obstacles. To leading order in $\bar{c} \ll 1$ the two agree for intermediate values of l.

The averaged flow permeability for the distribution of assemblages is obtained in several cases. If

$$R \ll (\ln \phi^{-1})^{-1} \quad (42)$$

the resistance within the assemblage is so weak that the flow is only perturbed slightly. Then

$$\alpha_0 \sim \frac{10\mu\phi}{3r^2}\left\langle \frac{c}{\ln (lr^{-1})} \right\rangle_I = \frac{10\mu\phi\bar{c}}{3r^2 \ln (lr^{-1})} \quad (43)$$

as $\phi,\bar{c},R \ln \phi^{-1} \to 0$. This is the same flow resistance as for a homogeneous, isotropic distribution of side rods with volume fraction $\phi\bar{c}$. For the stronger resistance

$$(\ln \phi^{-1})^{-1} \ll R \ll 1 \quad (44)$$

we obtain

$$\alpha_0 = \frac{20\mu\phi}{3l^2 \ln \phi^{-1}}\left[1 + O\left((R \ln \phi^{-1})^{-1}, \frac{\ln \ln \phi^{-1}}{\ln \phi^{-1}}\right)\right] \quad (45)$$

as $\phi \to 0$. Comparing with (38), at leading order the assemblages behave like impermeable cylinders of radius l. The first error term gives the correction due to the finite internal resistance.

If $R \gg 1$, the assemblages also appear impermeable to leading order. The flow drops to zero across a thin layer within the outer boundary of the assemblage. The solution for this layer gives the first correction to the value for impermeable cylinders. There are two cases, according to the form of the side-rod orientation distribution. First, if the cylinders are constrained to lie perpendicular to the core, $\mathbf{K}$ tends to a nonzero value as the radial coordinate $\rho \to l$. Then

$$\alpha_0 = \frac{20\mu\phi}{3l^2 \ln \phi^{-1}}\left[1 - (2R)^{-1/2}[\ln \phi^{-1}]^{-1} + O\left(\frac{\ln \ln \phi^{-1}}{\ln \phi^{-1}}, \frac{\ln \ln \bar{c}^{-1}}{R^{1/2} \ln \phi^{-1} \ln \bar{c}^{-1}}\right)\right] \quad (46)$$

as $\phi,\bar{c},R^{-1} \to 0$. If the orientation distribution is continuous at $\hat{\mathbf{x}}\cdot\mathbf{m} = 0$, as $\rho \to l$ the elements of $\mathbf{K}$ tend to zero like $(1 - \rho l^{-1})^{1/2}$. Then

$$\alpha_0 = \frac{20\mu\phi}{3l^2 \ln \phi^{-1}}\left[1 - \frac{k}{\ln \phi^{-1}}\left[\frac{\ln (\bar{c}^{-1}R^{1/5})}{PR \ln \bar{c}^{-1}}\right]^{2/5} + O\left(\frac{\ln \ln \phi^{-1}}{\ln \phi^{-1}}, \frac{\ln \ln \bar{c}^{-1}}{\ln \phi^{-1} \ln \bar{c}^{-1}}\left[\frac{\ln (\bar{c}^{-1}R^{1/5})}{R \ln \bar{c}^{-1}}\right]^{2/5}\right)\right] \quad (47)$$

as $\phi,\bar{c},R^{-1} \to 0$, where k and P are defined as follows. In the notation of section 2, $P = q(\mathbf{m})$ for $\hat{\mathbf{x}}\cdot\mathbf{m} = 0$; i.e., P is the orientation probability density function evaluated when $\mathbf{m}$ is perpendicular to the core. The constant k can be expressed as $-y(0)/y'(0)$, where $y(x)$ satisfies $y'' = x^{1/2}y$, with $y \to 0$ as $x \to \infty$. Numerical integration gives $k = 1.240...$

The effect of aggregation is evaluated by comparison with the averaged flow resistance in a homogeneous, isotropic distribution of side rods with volume fraction $\phi\bar{c}$, for which

$$\alpha_0 \sim \begin{cases} \dfrac{10\mu\phi\bar{c}}{3r^2 \ln (lr^{-1})} & \text{for } nl\phi \ll \ln (\phi\bar{c})^{-1} \\ \dfrac{20\mu\phi\bar{c}}{3r^2 \ln (\phi\bar{c})^{-1}} & \text{for } nl\phi \gg \ln (\phi\bar{c})^{-1} \end{cases} \quad (48)$$

as $\phi\bar{c},rl^{-1} \to 0$. Comparing (43), (45), and (48), there are two possibilities. If $nl \ln \phi^{-1} \ll \ln \bar{c}^{-1}$, the assemblages are so sparse that the side rods behave as independent obstacles, and to leading order the flow resistance is the same whether the rods are aggregated or not. If $nl \ln \phi^{-1} \gg \ln \bar{c}^{-1}$, the assemblages appear impermeable to flow at leading order and give a much smaller flow resistance than the homogeneous distribution of side rods with the same volume fraction.

5. Discussion

In this study we calculate averaged transport properties of random distributions of assemblages of cylinders with small volume fraction, as a model for dilute solutions of aggregated biopolymers. In the model assemblage (Figure 2), the side rods, cylinders of length l, are attached to a straight line at random points with uniform number density n. In section 2 the effect on the orientation distribution of the side rods due to steric interactions is considered for cylinders of arbitrary convex cross section. Averaged solute diffusivity and flow permeability are calculated in sections 3 and 4 for circular cylinders of radius r. Both the volume fraction $\bar{c}$ occupied by side rods within each assemblage and the volume fraction ϕ occupied by assemblages are assumed small throughout.

We do not consider the nonlinear interaction between flow and diffusion studied by Koch and Brady,[10] since in biopolymer solutions it is significant only at very low polymer concentrations. For example, in a chondroitin sulfate solution with a flow rate of 10^{-6} ms^{-1}, the interaction would be significant at polymer concentrations below about 10^{-3} mg mL^{-1}, whereas typical experimental concentrations are 10^3 times bigger.[15]

For diffusion and flow, the effect of aggregation is investigated by comparing a distribution of assemblages and a homogeneous distribution of side rods occupying the same overall volume fraction. The present theory assumes the volume fraction of assemblages is small; note that at concentrations where assemblages overlap strongly, the distribution of side rods is nearly homogeneous and aggregation will have little effect. We apply our results to dilute proteoglycan (PG) solutions, comparing (i) a solution of PG monomers and a solution of GAGs and (ii) a solution of PG aggregates and a solution of PG monomers. In the first case, the assemblage represents a PG monomer and in the second a PG aggregate. Note that there is no contribution at leading order from the core protein in the first case or the hyaluronate in the second. Table I gives the physical parameters for the two stages of aggregation, including the (molar) polymer concentration (C_p) at which the overall side-rod volume fraction is equal

Table I
Physical Parameters for the Two Stages of Aggregation of Proteoglycans[a]

	first stage: GAG → PG monomer	second stage: PG monomer → PG aggregate
n, nm^{-1}	0.5	0.05
r, nm	0.5	40
l, nm	40	300
$\bar{c}$	3×10^{-3}	0.27
δ	4.0	2.2
R	3.0	11.5
(C_p), mg mL^{-1}	2.3	0.6

[a] We give the number density of attachment points n, the side-rod radius r, and length l, the volume fraction $\bar{c}$ of an isolated assemblage occupied by side rods, the parameter δ for side-rod steric interactions (eq 7), the dimensionless flow resistance R (eq 41), and the polymer concentration (C_p) at which the overall side-rod volume fraction is equal to $\bar{c}$. The parameters for the first stage are based on data for chondroitin sulfate side chains.

Table II
Parameters for the First Stage of Aggregation at Different Values of the Added Salt Concentration (C_s)[a]

(C_s), M	λ, nm	$r + \lambda$, nm	$\bar{c}$	δ	R
(no charge)		0.5	3×10^{-3}	4.0	3
1	0.3	0.8	8×10^{-3}	5.2	4
0.1	1.0	1.5	3×10^{-2}	6.8	6
0.01	3.0	3.5	2×10^{-1}		12
0.001	10	10.5	">1"		

[a] We give the Debye length (or double-layer thickness) λ (eq 49), an increased GAG radius $r + \lambda$, the mean volume fraction $\bar{c}$ occupied by GAGs and their ionic atmospheres within an assemblage, and δ and R based on $r + \lambda$.

to $\bar{c}$; for much smaller concentrations ϕ is small, and for much larger concentrations the assemblages overlap strongly. Note that (C_p) is much smaller for a solution of PG aggregates than for one of PG monomers.

Since the GAGs are highly charged, they are surrounded by ionic double layers whose length scale is the Debye length λ. If the polymer solution is in equilibrium with a univalent salt solution with molar concentration (C_s), this is

$$\lambda = \left(\frac{\epsilon kT}{10^3 e^2 N_A (C_s)}\right)^{1/2} \tag{49}$$

where ϵ is the permittivity of the solvent, kT is the Boltzmann temperature, e is the electronic charge, and N_A is Avogadro's number. As the values of λ given in Table II show, electrostatic effects are important on the scale of the GAGs but not on the scale of PG monomers. The presence of charge causes repulsive forces between GAGs and increases the resistance to flow but can either increase or decrease the diffusivity of a charged solute.[16] A crude idea of electrostatic effects on side-rod interactions and flow permeability can be obtained by increasing the cylinder radius r by λ. The dimensionless parameters based on $r + \lambda$ are given in Table II for various salt concentrations.

The strength of steric interactions between side chains is determined by the size of the parameter δ defined by (7). Since this is greater than unity even in the absence of charge (Table I), the GAG chains should tend to lie perpendicular to the core, and this tendency should be strengthened by electrostatic repulsion.

To first order in the small volume fraction the point-solute diffusivity, derived in section 3, is unaffected by aggregation provided $\bar{c} \ll 1$. As Table I shows, this is a good approximation for PG monomers, but not so good for PG aggregates.

For a spherical solute whose radius $\mathcal{R}$ satisfies (28), section 3.3 predicts a larger effective diffusivity in the aggregated distribution. For the comparison between GAGs and PG monomers, this requires $\mathcal{R}$ to be well within the interval between 9 nm and $\min(9\phi^{-1/2},40)$ nm, and for the comparison between PG monomers and PG aggregates, well within the interval between 80 nm and $\min(80\phi^{-1/2},300)$ nm. Note that the empirical theory of Ogston et al.[12] for the diffusion of a spherical solute in a distribution of cylinders does not have the correct behavior in the limit when the effect of the cylinders is small.

In section 4, flow permeability is calculated for a distribution of fixed assemblages. The comparison with a homogeneous distribution of side rods depends on the size of the dimensionless flow resistance R defined by (41). If $R \ln \phi^{-1} \ll 1$, the side rods appear isolated at leading order and the averaged flow permeability is unaffected by aggregation. If $R \ln \phi^{-1} \gg 1$ the assemblages are impermeable at leading order and the averaged flow permeability is increased by aggregation. For both PG aggregates and PG monomers, R is greater than unity (Table I), so in sufficiently dilute solutions aggregation should decrease the flow resistance.

Although these conclusions are based on an idealized model, they are expected to remain broadly unchanged under more general conditions. For example, although the diffusion and flow calculations are for circular cylinders, when the side rods have arbitrary convex cross section similar scalings are expected, with r replaced by an effective radius $r = s/2\pi$, where s is the perimeter of the cross section. For small-ion diffusion, though the results of section 3 no longer apply if the side rods are charged, the diffusivity will be unaffected by aggregation provided the volume fraction occupied by side rods and double layers within the assemblage is small (see Table II). In PG solutions, aggregation is expected to reduce the flow resistance since the assemblages are nearly impermeable to flow. If the volume fraction $\bar{c}$ is not small, further reducing the internal flow, the same conclusion will apply. One refinement would be to allow the components of the assemblage to be flexible.[17,18]

Acknowledgment. C.G.P. gratefully acknowledges his support by a fellowship funded by Johnson and Johnson. We also wish to acknowledge very helpful discussions with Drs. K. H. Parker and C. P. Winlove of the Physiological Flow Studies Unit, Imperial College.

Appendix: Effective Diffusion Coefficient in a Distribution of Cylinders

Equation 15 gives the effective diffusivity, as far as the c term, in a distribution of circular cylinders with small volume fraction c, with an arbitrary orientation distribution and arbitrary uniform internal diffusivity d. The results for impermeable cylinders are (17) (arbitrary orientation distribution) and (18) (isotropic orientation distributions). This Appendix gives other special cases of (15) together with the c^2 term for aligned cylinders.[8]

For an isotropic orientation distribution, $\langle \mathbf{mm} \rangle$ is isotropic with a trace of 1, so $\langle \mathbf{mm} \rangle = (1/3)\mathbf{1}$. Therefore

$$\mathbf{D}_e = \left(1 + \frac{(d-1)(d+5)}{3(d+1)}c + O(c^2)\right)\mathbf{1} \tag{A1}$$

as $c \to 0$, in agreement with Koch and Brady's[10] equation (11).

When the cylinder axes are parallel to a unit vector $\mathbf{m}_0$, $\langle \mathbf{mm} \rangle = \mathbf{m}_0\mathbf{m}_0$. The effective diffusivity $\mathbf{D}_e$ depends

on two parameters: one for parallel diffusion

$$D_{\parallel} = 1 + (d-1)c \tag{A2}$$

which is exact for all c, and another for transverse diffusion

$$D_{\perp} = 1 + \frac{2(d-1)}{(d+1)}c + O(c^2) \tag{A3}$$

as $c \to 0$. These equations agree with earlier results.[8,10]

The c^2 correction depends on the solution for diffusion past two cylinders, which is not known for arbitrary orientation distributions. For parallel cylinders, however, Peterson and Hermans[8] give the c^2 contribution to $D_{\perp}$ (cf. Howells'[7] calculation of the flow permeability in a distribution of parallel cylinders). Putting $b = (1 - d)/(1 + d)$, this gives

$$D_{\perp} = 1 - 2bc + 2(b^2 - 8bA(b))c^2 + O(c^3) \tag{A4}$$

as $c \to 0$, where

$$A(b) = \frac{1}{2}\int_0^{\infty} \sinh 2\xi \left[-1 + 4\sum_{n=1}^{\infty} \frac{n \sinh^2 \xi}{e^{2n\xi} - b^2 e^{-2n\xi}} \right] d\xi \tag{A5}$$

For impermeable cylinders, when $b = 1$, numerical integration of $A(b)$ to four significant figures gives

$$D_{\perp} = 1 - 2c + 1.255c^2 + O(c^3) \tag{A6}$$

as $c \to 0$. Numerical values for other cases are given by Peterson and Hermans.[8]

References and Notes

(1) Grodzinsky, A. J. *CRC Crit. Rev. Biomed. Eng.* **1983**, *9*, 133-199.
(2) Hardingham, T. E.; Muir, H.; Kwan, M. K.; Lai, W. M.; Mow, V. C. *J. Orthop. Res.* **1987**, *5*, 36-46.
(3) Happel, J. *AIChE J.* **1959**, *5*, 174-177.
(4) Kuwabara, S. *J. Phys. Soc. Jpn.* **1959**, *14*, 527-532.
(5) Nilsson, L. G.; Nordenskiold, L.; Stilbs, P.; Braunlin, W. H. *J. Phys. Chem.* **1985**, *89*, 3385-3391.
(6) Hinch, E. J. *J. Fluid Mech.* **1977**, *83*, 695-720.
(7) Howells, I. D. *J. Fluid Mech.* **1974**, *64*, 449-475.
(8) Peterson, J. M.; Hermans, J. J. *J. Compos. Mater.* **1969**, *3*, 338-354.
(9) Cametti, C.; Di Basio, A. *Ber. Bunsenges. Phys. Chem.* **1986**, *90*, 621-625.
(10) Koch, D. L.; Brady, J. F. *AIChE J.* **1986**, *32*, 575-591.
(11) Santaló, L. A. *Integral Geometry and Geometric Probability*; Addison-Wesley: Reading, MA, 1976; Vol. 1.
(12) Ogston, A. G.; Preston, B. N.; Wells, J. D. *Proc. R. Soc. London A* **1973**, *333*, 297-316.
(13) Spielman, L.; Goren, S. L. *Environ. Sci. Technol.* **1968**, *2*, 279-287.
(14) Batchelor, G. K. *J. Fluid Mech.* **1970**, *44*, 419-440.
(15) Maroudas, A.; Weinberg, P. D.; Parker, K. H.; Winlove, C. P. *Biophys. Chem.* **1988**, *32*, 257-270.
(16) Phillips, C. G. Transport in Biological Tissue and in Shear Flow. Ph.D. Thesis, Cambridge University, 1987.
(17) Jansons, K. M.; Phillips, C. G. On the Application of Geometric Probability Theory to Polymer Networks and Suspensions. I. *J. Colloid Interface Sci.*, accepted for publication.
(18) Jansons, K. M.; Phillips, C. G. On the Application of Geometric Probability Theory to Polymer Networks and Suspensions. II. In preparation.

Polymer Self-Diffusion in Ternary Solutions and the Monomer and Segmental Self-Diffusion Coefficients

D. N. Pinder

Physics and Biophysics Department, Massey University, Palmerston North, New Zealand.

Received July 19, 1989; Revised Manuscript Received August 23, 1989

ABSTRACT: The monomer self-diffusion coefficient of polystyrene in Θ and non-Θ solutions is determined as a function of concentration. Also the concentration dependence of the segmental self-diffusion coefficient (which includes hydrodynamic screening effects) is measured for polystyrenes in non-Θ solutions. These two quantities are shown to be distinct. The self-diffusion coefficients of polystyrenes in semidilute non-Θ solutions have been corrected by using both the monomer and the segmental self-diffusion coefficients, and these corrected data have been compared with the scaling laws and with the theory of Hess. This theory, which applies to non-Θ solutions with concentrations less than the crossover concentration, is shown to be in agreement with the data for concentrations close to the overlap concentration, for larger concentrations the data decreases faster than theory would allow.

Introduction

The dynamical behavior of polymer chains at concentrations close to and above the coil overlap concentration, c^*, has excited considerable interest. Theories have been developed to describe the behavior, and various experimental procedures have been applied to measure the dynamical parameters. The self-diffusion coefficient, D_s, has proved to be a particularly useful dynamical property for investigating the motion of a single chain among others in semidilute solutions.

Major theoretical developments were engendered by the scaling and reptation models proposed by de Gennes[1,2] based on the concept of the "effective tube" originally introduced by Edwards.[3] Theories based on these models assume that in semidilute solutions the impediment to motion of a single chain is caused by chain entanglements; no account is taken of any increase in monomer friction coefficient as the polymer concentration increases. These theories predict the simple scaling laws

$$D_s \sim M^{-2}c^{-1.75} \quad \text{for non-}\Theta\text{ solutions}$$

$$D_s \sim M^{-2}c^{-3} \quad \text{for }\Theta\text{ solutions}$$

where M is the polymer molar mass and c the polymer concentration.

The scaling theory for non-Θ solutions has been extended to include the concept of the concentration crossover. This modification accounts for the behavior of real non-Θ solu-

0024-9297/90/2223-1724$02.50/0